Title
Local progression kinetics of macular atrophy in recessive Stargardt disease.

Journal
Ophthalmic Genetics, 44(6)

Authors
Young, Benjamin
Zhao, Peter
Shen, Liangbo
et al.

Publication Date
2023-12-01

DOI
10.1080/13816810.2023.2228891

Peer reviewed

HHS Public Access
Author manuscript
Ophthalmic Genet. Author manuscript; available in PMC 2024 December 01.

Published in final edited form as:
Ophthalmic Genet. 2023 December ; 44(6): 539–546. doi:10.1080/13816810.2023.2228891.

Local Progression Kinetics of Macular Atrophy in Recessive Stargardt Disease

Benjamin Young, MD, MS[1], **Peter Y. Zhao, MD**[2], **Liangbo L. Shen, MD**[3], **Abigail Fahim, MD, PhD**[4], **Thiran Jayasundera, MD**[4]

[1]Department of Ophthalmology, Oregon Health & Sciences University, Portland, OR USA

[2]Department of Ophthalmology, Tufts University School of Medicine, Boston, MA USA

[3]Department of Ophthalmology, University of California San Francisco, San Francisco, CA USA

[4]Department of Ophthalmology and Visual Sciences, University of Michigan Medical School, Ann Arbor, MI USA

Abstract

Background: To determine the effect of lesion topography on progression in Stargardt disease (STGD1).

Methods: Fundus autofluoresence (excitation 488nm) images of 193 eyes in patients with proven *ABCA4* mutation were semi-automatically segmented for autofluoresence changes: (DDAF) and questionably decreased autofluoresence (QDAF), which are proxies for retinal pigment epithelial (RPE) atrophy. We calculated topographic incidence of DDAF and DDAF + QDAF, as well as velocity of progression of the border of lesions using Euclidean distance mapping.

Results: Incidence of atrophy was highest near the fovea, then decreased in incidence with increased foveal eccentricity. However, the rate of atrophy progression followed the opposite pattern; rate of atrophy increased with distance from foveal center. The mean growth rate 500 microns from the foveal center for DDAF + QDAF was 39 microns per year (95% CI = 28–49), whereas the mean growth rate 3000 microns from the foveal center was 342 microns per year (95% CI = 194–522). No difference in growth rate was noted by axis around the fovea.

Conclusions: Incidence and progression of atrophy by fundus autofluorescence follow opposite patterns in STGD1. Further, atrophy progression increases significantly with distance from foveal center, which should be taken into consideration in clinical trials.

Keywords

Macular Atrophy; Stargardt Disease; Progression Kinetics

Corresponding Author: Thiran Jayasundera, MD, W.K. Kellogg Eye Center, Department of Ophthalmology and Visual Sciences, 1000 Wall Street, Ann Arbor, MI 48105, thiran@med.umich.edu.

Declaration of Interest: The authors report there are no competing interests to declare.

Disclaimer: The views expressed in this article are those of the authors and do not necessarily reflect the position or policy of the University of Michigan Medical School.

Conflicts of Interest: The authors report no conflicts of interest.

Autosomal-recessive Stargardt disease (STGD1) is the most common cause of juvenile macular degeneration, caused by pathogenic variants in the *ABCA4* gene.[1] It is characterized by areas of outer retinal atrophy, representing loss of photoreceptors and retinal pigment epithelium (RPE), which expand over time with disease progression. When the fovea is affected, visual acuity is decreased, leading to significant loss of quality of life and functional impairment.[2–4] Extrafoveal atrophy may also cause visual dysfunction through paracentral scotomas in the visual field or decreased contrast sensitivity.[5]

Significant research activity has been dedicated to slowing the natural history of STGD1, with proposed therapies including pharmacotherapies and gene therapy.[1, 6] Potential outcome measures to assess efficacy of treatments under development include functional outcomes such as retinal sensitivity on microperimetry, and imaging outcomes such as changes in the area or location of the border of atrophy, since progression of atrophy observed on fundus autofluorescence (FAF) corresponds to loss of functional retinal tissue and scotomas in STGD1.[2–4, 7–9]

In a meta-analysis of 564 eyes with STGD1 from 7 studies, it has been shown that atrophic lesions in STGD1 grow in relation to their effective radius, defined as square root of [lesion area / π], rather than total area.[10] Since the effective radius of a lesion is directly proportional to its perimeter, areas of RPE atrophy in STGD1 essentially grow linearly by their perimeter; in other words, disease activity occurs at the wavefront of disease at the lesion edge. However, it is not known whether distance from the fovea affects the incidence of atrophic lesions or their rate of growth.

In this report, we investigate whether there is topographic variation in the incidence and growth of atrophy in STGD1 by examining a cohort of patients with mutation-proven STGD1 and known macular atrophy using FAF images.

Materials and Methods

This study was a retrospective analysis of patients seen at the Kellogg Eye Center from 2010 to 2020. We included patients for whom 1) a clinical diagnosis of STGD1 was established by a fellowship-trained inherited retinal dystrophy (IRD) specialist, 2) molecular confirmation of the clinical diagnosis was obtained via genetic testing and identification of 2 pathogenic or likely pathogenic variants in *ABCA4* through a Clinical Laboratory Improvement Amendments (CLIA)-certified laboratory, and 3) high-resolution fundus autofluoresence (excitation 488nm) images were obtained with an Optos California camera (Optos PLC, Dunfermline, Scotland, UK) for one or more time points. Exclusion criteria included lack of imaging, or significant media opacity obscuring imaging. No specific exclusions were made to previously described pattern subtypes of STGD1, such as foveal sparing, or multifocal lesions. To allow precise measurement of lesion size, images were projected onto a curved surface with an assumed nominal eye diameter of 24 millimeters using proprietary Optos research software previously described in detail elsewhere.[11] Images were then rotated and warped for alignment using 4 vessel crossing points as anchors using the Open Computer Vision 2 (OpenCV2) package’s “getPerspective” and “warpPerspective” functions.[12]

Images were segmented, or in other words delineated, in a semi-automated manner using Photoshop v23.5 (Adobe Inc, San Jose CA, USA), with the "Magic Wand" tool". The segmentation layer was drawn using the Magic Wand tool to automatically identify regions of interest congruent with user-selected features. Then, these regions were manually edited in Photoshop if necessary, by the grader. Two different types of regions of interest were documented per image: "definitely decreased autofluorescence" (DDAF), where an area is at least 90% as dark as a reference value (the optic disc), and areas of "questionably decreased autofluorescence" (QDAF), where an area is between 50–90% as dark as the optic disc, as initially defined by the ProgSTAR group.[13] Segmentation was performed by an IRD-trained retina specialist (PYZ) who was masked to the research hypothesis at the time of segmentation. For reliability testing, a second trained retina specialist (BKY) performed segmentations in a random sample of 20% of images (n=59). Dice coefficients, defined as area of overlap between graders multiplied by 2 divided by the total area segmented by each grader were calculated for both DDAF and DDAF+QDAF regions, where a value of 1 indicates perfect agreement.[14, 15]

Segmentations were then converted to binary masks using Python 4.1 in the Anaconda scientific environment. Masks of left eye images were mirrored so they would have the same directional orientation as right eye images. Then, all masks of DDAF and QDAF + DDAF were summed. A mean pixel density was calculated to determine the average distribution of atrophy over all patients. The probability of having atrophy at each distance from the foveal center over all images was calculated, along with 95% confidence intervals. Next, masks were compared for progression using a previously described technique using the construction of Euclidean distance maps.[15] In brief, masks were converted to contours describing the boundary of edges using the "FindContours" function in the OpenCV2 library. Then, each point on the contour of a preceding visit was compared to a map of minimum Euclidean distance from points of the antecedent visit. This minimum distance to approach the antecedent point was then divided by the time progressed to determine the local velocity of atrophy at that point.

All such data points were summed and used to generate a profile of mean velocities by distance and axis around the foveal center, along with 95% confidence intervals for both DDAF and DDAF + QDAF masks.

The approval of the University of Michigan Institutional Review Board was obtained prior to initiation of this retrospective study. This study adhered to the tenets of the Declaration of Helsinki.

Results

193 eyes of 97 patients met inclusion criteria, with 296 total images available for analysis. 71 eyes of 36 patients had more than one visit, with 186 images available for longitudinal analysis. Average age of patients at baseline was 30.8 (SD = 17.1) and 53% were female. Of the patients with more than one visit, mean duration of follow-up was 30.6 (SD = 18.7) months, with 2.5 (SD = 0.7) visits. Mean logMAR visual acuity at baseline was 0.82 (SD =

0.52), and mean logMAR visual acuity at last follow-up among the longitudinal group was 0.91 (SD = 0.61).

Dice coefficients between the two graders were 0.89 +/− 0.13 for DDAF, and 0.76 +/− 0.21 for DDAF + QDAF, which demonstrates reliability of the segmentation method, and is in line with previous literature.[14–16]

Figure 1 shows heatmaps of topographic location for incidence of DDAF alone, and incidence of DDAF + QDAF. Figure 2 shows the likelihood of incident DDAF and DDAF + QDAF by distance from the foveal center, demonstrating that incidence of atrophy is higher at the foveal center, and then decreases in likelihood away from the foveal center. Figure 3 shows heatmaps of the rate of lesion progression for DDAF alone and DDAF + QDAF. Figure 4 demonstrates that the rate of atrophy progression is slower near the foveal center, and faster further from the foveal center. To illustrate this, the mean growth rate 500 microns from the foveal center for DDAF + QDAF was 39 microns per year (95% CI = 28–49), whereas the mean growth rate 3000 microns from the foveal center was 342 microns per year (95% CI = 194–522). Figure 4 shows the rate of atrophy progression with respect to rotational axis around the foveal center, where zero degrees represents directly nasal. No statistically significant variation in rate of atrophy progression by axis was found.

Discussion

In this cohort, the rate of atrophy progression varies in STGD1 significantly depending on distance from the foveal center; an 8.8-fold difference in progression rate between 500 microns to 3000 microns from the foveal center (approximately the edge of the macula). This finding has substantial impact on design of clinical trials that are utilizing the progression of atrophic lesions as an outcome measure. Our results show that it is necessary to account for topographic variation in study design. We also demonstrate that areas of incident RPE atrophy are not randomly distributed, but rather clustered near the fovea. Taken together, these findings suggest that most atrophy progression will be small and near the fovea, making detection of changes in atrophic area more difficult. We did not find a difference in atrophy growth rate based on rotational axis around the fovea.

Analysis of both DDAF lesions alone and DDAF + QDAF lesions together showed similar patterns of atrophy progression. QDAF has been proposed to possibly represent the early stages of disease or retina at risk of converting into DDAF, and therefore more likely to be treatable by therapies that prevent progression.[17] Hence, understanding the kinetics of both DDAF and QDAF are important when planning clinical trials.

Our group previously performed a similar analysis on a cohort of patients with age-related macular degeneration (AMD) from the Age-Related Eye Disease Study (AREDS).[15] Interestingly, although the molecular pathophysiology, patient age, and patient demographics of AMD and STGD1 differ substantially, the kinetics of atrophic lesion incidence and progression show similar patterns of increased lesion incidence closer the fovea, and increased rate of lesion progression further from the fovea. Despite the substantial differences in cause of disease in AMD and STGD1, our analyses taken together suggest that once the RPE becomes significantly affected by the underlying disease process, there may be similar end mechanisms responsible for outer retinal atrophy progression. There have been proposed shared pathways in the two diseases previously, such as photooxidative stress, but a unifying mechanism has not been described.[18] Additionally, the demonstration that the topographic curves of atrophy incidence and atrophy progression sharply contrast may suggest that different processes are involved in the initiation of atrophy versus the growth of existing atrophy. While this study cannot elucidate the exact cell- and tissue-level mechanisms responsible, it establishes a question worthy of further investigation in the laboratory setting across different causes of RPE disease. Further, these similar findings may explain similarities in ovoid, fovea sparing atrophy which are sometimes observed in both diseases; these may occur because atrophy rate towards the foveal center decreases.

The findings described here contribute further to the understanding of atrophic lesion growth beyond that published by the ProgStar study group.[17] In the ProgStar data, lesion growth rate by area (mm^2) was dependent on the initial lesion size. However, atrophy perimeter growth rate (mm) was not examined. Based on our analysis, larger initial lesions are more likely to be in the peripheral macula, which would explain the more rapid lesion growth rate. The interaction between initial lesion size and lesion topography requires further study. A more thorough understanding of the natural history of lesion incidence and growth kinetics would facilitate better design of clinical trials to demonstrate efficacy of potential therapeutics. Further, others have qualitatively described early changes in autofluoresence in the parafovea.[19] This study quantitatively shows the highest incidence of DDAF near and involving the fovea. Here, we did not exclude patients or images where the fovea was already involved. Further quantitative study of early autofluoresence changes in STGD1 are warranted.

Others have also shown that rod and cone loss may increase exponentially after an initial plateau phase.[20] While this study is not directly reflective of photoreceptor loss, it may provide some explanation for this finding. The plateau phase may correlate to the period prior to DDAF onset, or early DDAF. Then, as lesions which start near the parafovea expand outwards, the rate of atrophy progression increases at a proportionally greater rate, which may produce exponential data, though this study cannot confirm this. Our group has observed the opposite in choroideremia, where peripheral lesions decrease in progression velocity as they approach the fovea, which produces an exponentially decreasing rate of RPE loss.[21,22]

One limitation of this study is the use of autofluorescence imaging for identification of areas of RPE atrophy. However, as previously discussed, FAF is an accepted modality of monitoring outer retinal loss in STGD1.[13] Ideally, multi-modal imaging data, including OCT features such as EZ loss, hypertransmission, or near-infrared autofluoresence, could be used to confirm the borders of DDAF and QDAF lesions. Further, other devices for autofluoresence imaging, such as Heidelberg systems, may demonstrate different quality of image production, which could reduce comparability of this study compared to others investigating changes in autofluoresence. Also, others have suggested QDAF may have high variability, especially between imaging modalities, which may limit our DDAF+QDAF analysis.[23] This study also had a relatively small sample size, and although our results were statistically significant, validating the results with a larger data set would help confirm the findings. Further, the retrospective design may limit the quality of data, as it is possible that patients with faster or slower rates of atrophy may have had differences in likelihood for follow-up, creating selection bias. Also, return intervals were not predetermined as in a prospective study, but were rather determined by routine clinical care and patient availability. We also relied on segmentation of lesions by a single IRD-fellowship trained expert. However, prior studies have shown that segmentation of FAF images is reliable with high inter-grader agreement, especially for DDAF lesions.[24] Optical coherence tomography may have been helpful in segmentation of lesions, but was not available for all patients, so was not used for uniformity. The local atrophy expansion rate is an objective measure to quantify the linear expansion rate of lesions, but may not be reliable for regions where lesion margins merge or progress along non-linear paths.

In conclusion, we quantified the topography of incidence and progression rate of autofluorescence changes in 193 eyes of 97 patients with STGD1. To our knowledge, this is the first study which demonstrates that the rate of atrophy increases with distance from the foveal center in STGD1, a similar pattern as is seen in geographic atrophy in age-related macular degeneration.[15] Given this pattern is opposite of that of the incidence of autofluorescence lesions, these findings suggest that there may be mechanistic differences forces driving initiation and progression of lesions. These natural history findings may improve selection of endpoints in clinical trials, and provide insight into the mechanisms of atrophy in STGD1.

Funding/Support:

This work was supported in part by the Heed Ophthalmic Foundation. This funding organization was not involved with the design and conduct of the study; collection, management, analysis, and interpretation of the data; preparation, review, or approval of the manuscript; or decision to submit the manuscript for publication.

Data Availability Statement:

The participants of this study did not give written consent for their data to be shared publicly, so due to the sensitive nature of the research supporting data is not available.

References

1. Tanna P, Strauss RW, Fujinami K, Michaelides M. Stargardt disease: clinical features, molecular genetics, animal models and therapeutic options. Br J Ophthalmol 2017;101(1):25–30. [PubMed: 27491360]
2. Sunness JS, Ifrah A, Wolf R, et al. Abnormal Visual Function Outside the Area of Atrophy Defined by Short-Wavelength Fundus Autofluorescence in Stargardt Disease. Invest Ophthalmol Vis Sci 2020;61(4):36.
3. Gomes NL, Greenstein VC, Carlson JN, et al. A comparison of fundus autofluorescence and retinal structure in patients with Stargardt disease. Investigative ophthalmology & visual science 2009;50(8):3953–9. [PubMed: 19324865]
4. Sunness JS, Steiner JN. Retinal function and loss of autofluorescence in stargardt disease. Retina 2008;28(6):794–800. [PubMed: 18536594]
5. Alahmadi BO, Omari AA, Abalem MF, et al. Contrast sensitivity deficits in patients with mutation-proven inherited retinal degenerations. BMC Ophthalmol 2018;18(1):313. [PubMed: 30526558]

6. Scholl HP, Strauss RW, Singh MS, et al. Emerging therapies for inherited retinal degeneration. Sci Transl Med 2016;8(368):368rv6.

7. Csaky KG, Richman EA, Ferris FL, 3rd. Report from the NEI/FDA Ophthalmic Clinical Trial Design and Endpoints Symposium. Invest Ophthalmol Vis Sci 2008;49(2):479–89. [PubMed: 18234989]

8. Schönbach EM, Strauss RW, Muñoz B, et al. Longitudinal Microperimetric Changes of Macular Sensitivity in Stargardt Disease After 12 Months: ProgStar Report No. 13. JAMA Ophthalmol 2020;138(7):772–9. [PubMed: 32463436]

9. Schönbach EM, Wolfson Y, Strauss RW, et al. Macular Sensitivity Measured With Microperimetry in Stargardt Disease in the Progression of Atrophy Secondary to Stargardt Disease (ProgStar) Study: Report No. 7. JAMA Ophthalmol 2017;135(7):696–703. [PubMed: 28542693]

10. Shen LL, Sun M, Grossetta Nardini HK, Del Priore LV. Natural History of Autosomal Recessive Stargardt Disease in Untreated Eyes: A Systematic Review and Meta-analysis of Study- and Individual-Level Data. Ophthalmology 2019;126(9):1288–96. [PubMed: 31227323]

11. Croft DE, van Hemert J, Wykoff CC, et al. Precise montaging and metric quantification of retinal surface area from ultra-widefield fundus photography and fluorescein angiography. Ophthalmic Surg Lasers Imaging Retina 2014;45(4):312–7. [PubMed: 25037013]

12. Bradski G The OpenCV Library. Dr Dobb's Journal of Software Tools. 2000.

13. Strauss RW, Ho A, Muñoz B, et al. The Natural History of the Progression of Atrophy Secondary to Stargardt Disease (ProgStar) Studies: Design and Baseline Characteristics: ProgStar Report No. 1. Ophthalmology 2016;123(4):817–28. [PubMed: 26786511]

14. Liefers B, Colijn JM, González-Gonzalo C, et al. A Deep Learning Model for Segmentation of Geographic Atrophy to Study Its Long-Term Natural History. Ophthalmology 2020;127(8):1086–96. [PubMed: 32197912]

15. Shen LL, Sun M, Ahluwalia A, et al. Local Progression Kinetics of Geographic Atrophy Depends Upon the Border Location. Invest Ophthalmol Vis Sci 2021;62(13):28.

16. Zhao PY, Branham K, Schlegel D, et al. Automated Segmentation of Autofluorescence Lesions in Stargardt Disease. Ophthalmol Retina 2022.

17. Strauss RW, Kong X, Ho A, et al. Progression of Stargardt Disease as Determined by Fundus Autofluorescence Over a 12-Month Period: ProgStar Report No. 11. JAMA Ophthalmol 2019;137(10):1134–45. [PubMed: 31369039]

18. Sears AE, Bernstein PS, Cideciyan AV, et al. Towards Treatment of Stargardt Disease: Workshop Organized and Sponsored by the Foundation Fighting Blindness. Transl Vis Sci Technol 2017;6(5):6.

19. Khan KN, Kasilian M, Mahroo OAR, Tanna P, Kalitzeos A, Robson AG, Tsunoda K, Iwata T, Moore AT, Fujinami K, Michaelides M. Early Patterns of Macular Degeneration in ABCA4-Associated Retinopathy. Ophthalmology. 2018 May;125(5):735–746. [PubMed: 29310964]

20. Cideciyan AV, Swider M, Aleman TS, Tsybovsky Y, Schwartz SB, Windsor EA, Roman AJ, Sumaroka A, Steinberg JD, Jacobson SG, Stone EM, Palczewski K. *ABCA4* disease progression and a proposed strategy for gene therapy. Hum Mol Genet. 2009 Mar 1;18(5):931–41. [PubMed: 19074458]

21. Shen LL, Ahluwalia A, Sun M, Young BK, Grossetta Nardini HK, Del Priore LV. Long-term Natural History of Atrophy in Eyes with Choroideremia-A Systematic Review and Meta-analysis of Individual-Level Data. Ophthalmol Retina. 2020 Aug;4(8):840–852. [PubMed: 32362554]

22. Young BK, Shen LL, Del Priore LV. An In Silica Model for RPE Loss Patterns in Choroideremia. Invest Ophthalmol Vis Sci. 2021 Nov 1;62(14):10.

23. Strauss RW, Muñoz B, Jha A, Ho A, Cideciyan AV, Kasilian ML, Wolfson Y, Sadda S, West S, Scholl HPN, Michaelides M. Comparison of Short-Wavelength Reduced-Illuminance and Conventional Autofluorescence Imaging in Stargardt Macular Dystrophy. Am J Ophthalmol. 2016 Aug;168:269–278. [PubMed: 27296491]

24. Domalpally A, Danis R, Agrón E, et al. Evaluation of Geographic Atrophy from Color Photographs and Fundus Autofluorescence Images: Age-Related Eye Disease Study 2 Report Number 11. Ophthalmology 2016;123(11):2401–7. [PubMed: 27448832]

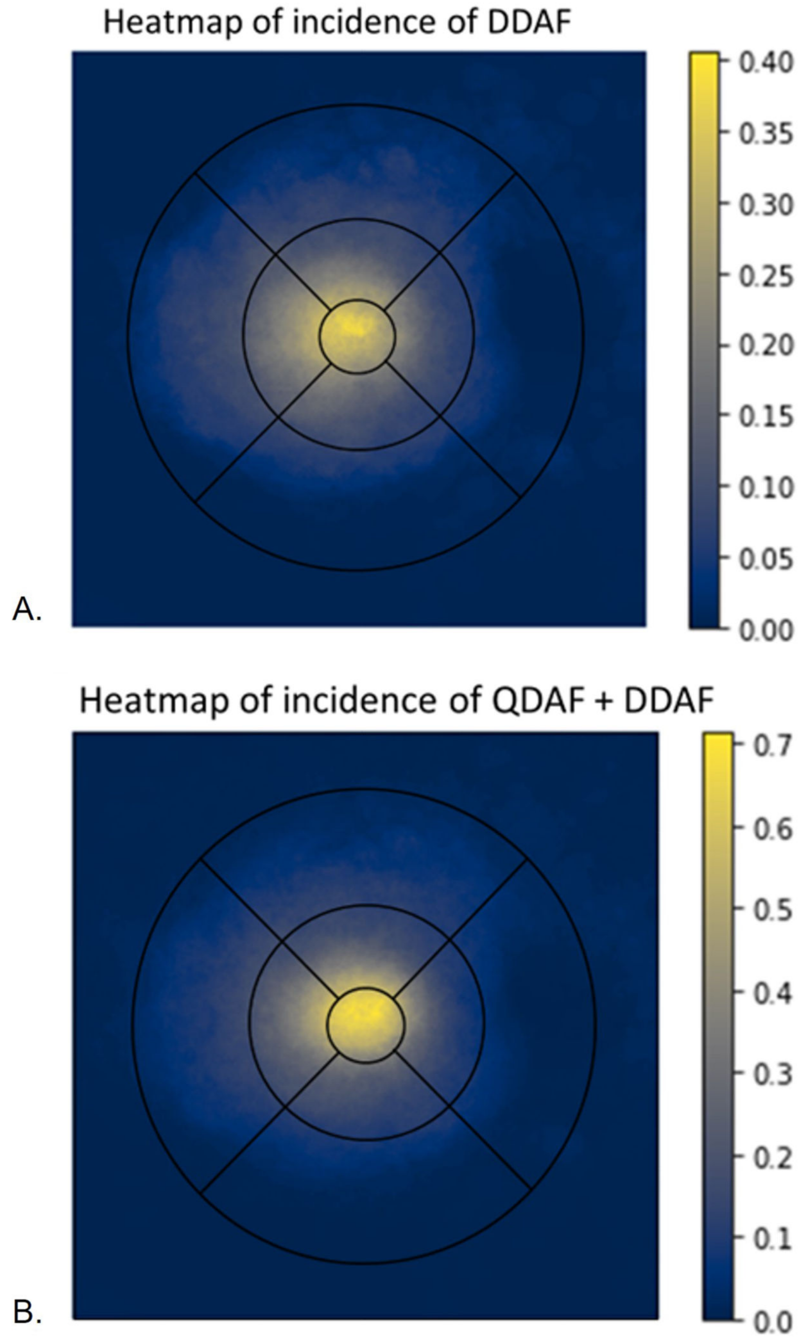

Figure 1.

Heatmaps of overall incidence of DDAF alone (A) and DDAF with QDAF (B). Incidence is higher closer to the foveal center. All left sided fundus photos were horizontally flipped to align with right sided fundus photos. A standard ETDRS grid is overlaid for scale, with 1, 3, and 6mm rings.

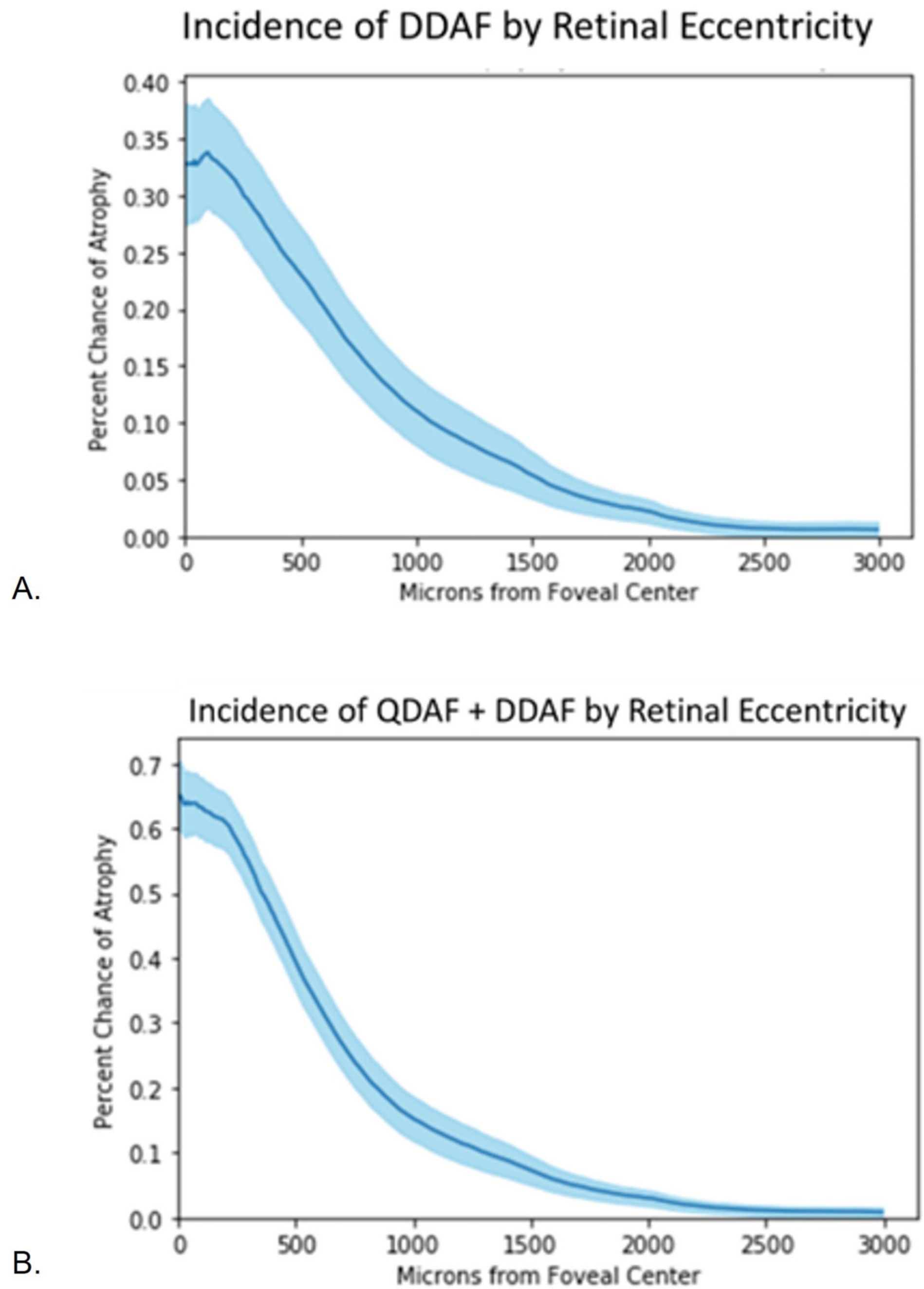

Figure 2.

Incidence of DDAF alone (A) and DDAF with QDAF by retinal eccentricity over all images in this analysis with macular atrophy. Light blue indicates 95% confidence intervals.

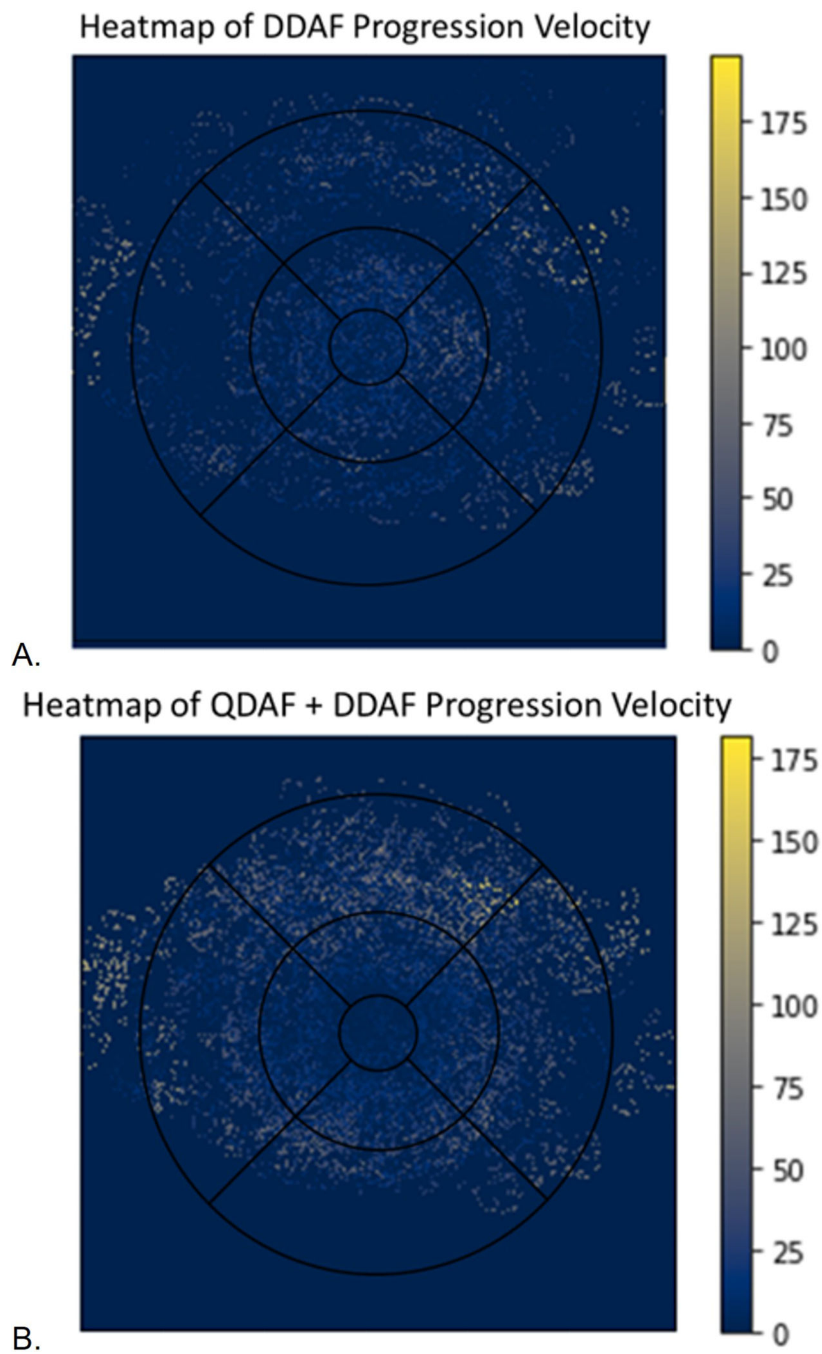

Figure 3.

Heatmaps demonstrating the velocity of atrophy progression at each topographic point by Euclidean Distance Maps for DDAF alone (A) and DDAF with QDAF (B). A value of zero indicates there was no atrophy progression noted at that point in the image dataset (ie atrophy may have been completely absent in that area). All left sided fundus photos were horizontally flipped to align with right sided fundus photos. A standard ETDRS grid is overlaid for scale, with 1, 3, and 6mm rings.

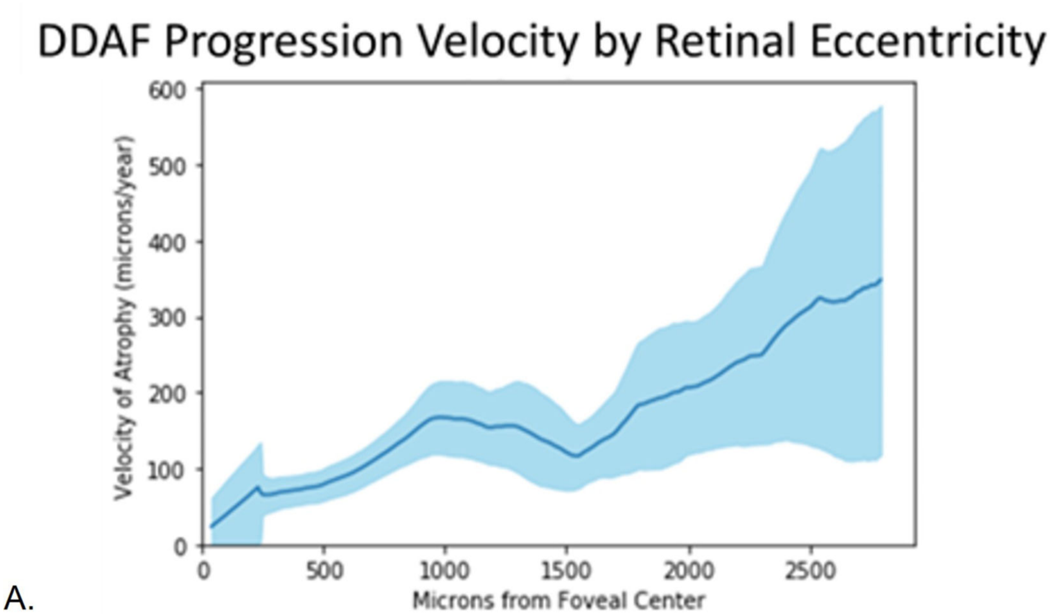

A.

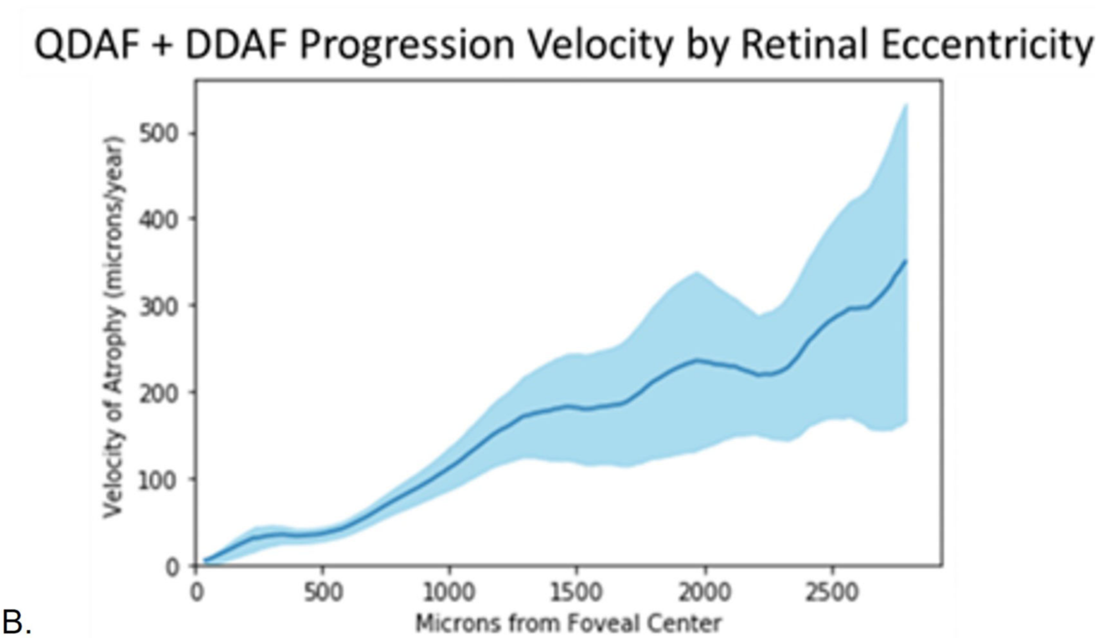

B.

Figure 4.

Mean velocity of atrophy progression by retinal eccentricity for DDAF alone (A) and DDAF with QDAF (B). Atrophy progresses more rapidly further from the foveal center. Light blue indicates 95% confidence intervals.

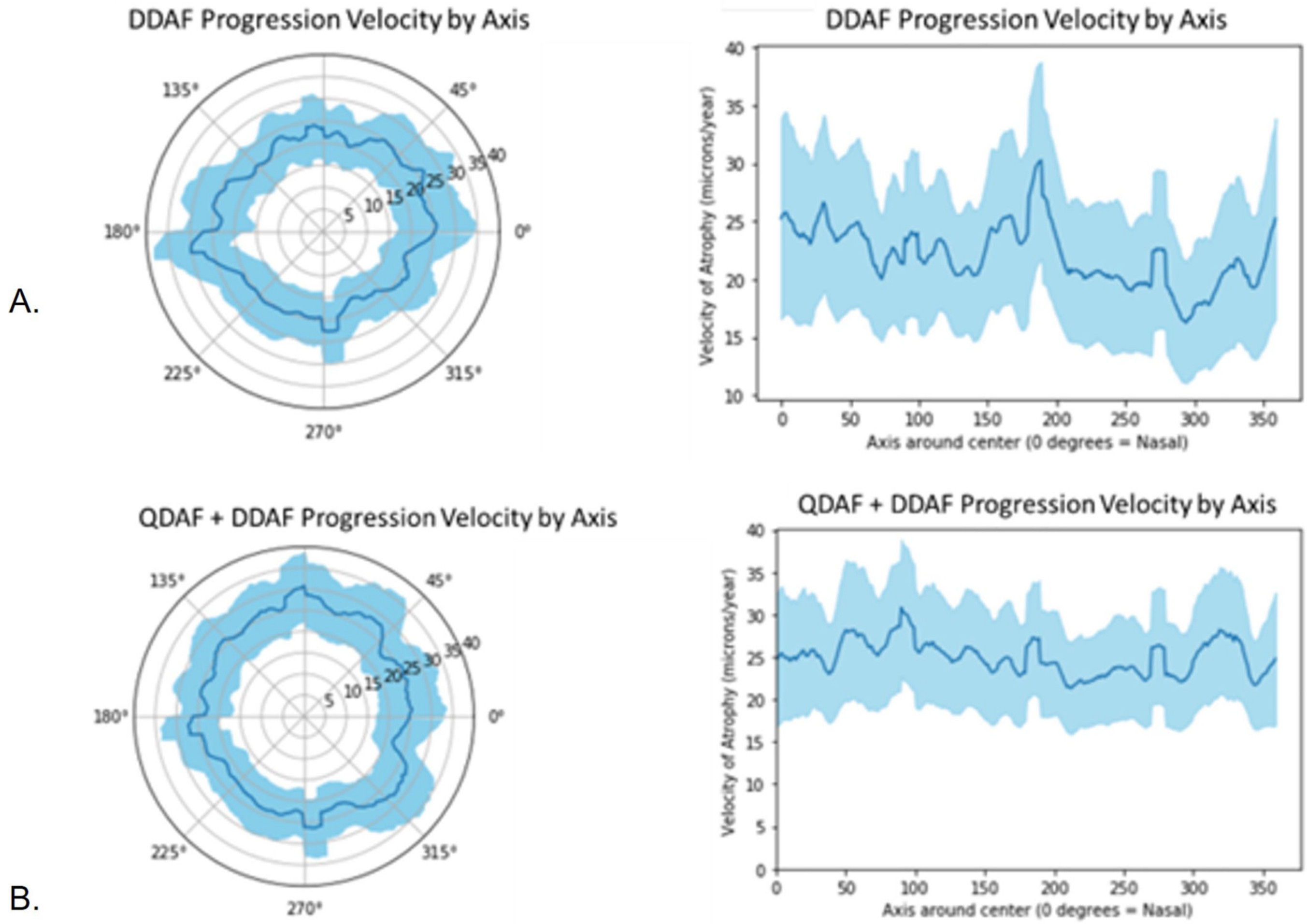

Figure 5.

Velocity of atrophy progression by topographic axis around the foveal center for DDAF alone (A) and DDAF with QDAF (B). There is no statistically significant variation in atrophy progression for any axis around the foveal center. Light blue indicates 95% confidence interval.